ELSEVIER

Journal of Non-Crystalline Solids 167 (1994) 295–306

JOURNAL OF NON-CRYSTALLINE SOLIDS

Pore structure evolution in silica gel during aging/drying. IV. Varying pore fluid pH §

Pamela J. Davis [a], Ravindra Deshpande [a], Douglas M. Smith [a,*], C. Jeffrey Brinker [a,b], Roger A. Assink [c]

[a] *UNM/NSF Center for Micro-Engineered Ceramics, University of New Mexico, Albuquerque, NM 87131, USA*
[b] *Division 1846, Sandia National Laboratories, Albuquerque, NM 87185, USA*
[c] *Division 1812, Sandia National Laboratories, Albuquerque, NM 87185, USA*

(Received 14 July 1993; revised manuscript received 10 August 1993)

Abstract

In an effort to understand the various phenomena which occur during aging of silica gels at different pH, silica particles prepared by three routes distinguished principally by their silicon coordination (Q^n distributions) (Stöber silica spheres, Ludox and Cab-O-Sil) were employed. In situ techniques were used including proton spin–lattice relaxation, SAXS and zeta potential for the wet state and ^{29}Si MAS-NMR, SEM, TEM and N_2 sorption for dry samples. In solution, the surface area increased in the following order after aging at pH 10 as compared with that at pH 7 and the initial dry surface area: Cab-O-Sil < Ludox ≪ Stöber which is inversely proportional to the degree of silicon coordination. This same trend was observed for the surface charge measurements. Surface areas calculated from ^{29}Si MAS-NMR for four different Stöber sphere sizes were of order 1000 m^2/g as compared with nitrogen/BET surface areas which varied from 9 to 370 m^2/g, indicating significant internal surface which is inaccessible to nitrogen. The ^{29}Si NMR results for the Stöber spheres were consistent with a close packed aggregate of ~3 nm primary particles. In addition to particulate silica, aging at varying pH of a two-step acid/base-catalyzed silica gel was studied. At all pH values, the surface area was higher in the wet gel as compared with the xerogel. Aging at higher pH was found to yield lower surface area, larger pore volume and a narrower pore size distribution depending upon the pH, aging time and surface tension of the final pore fluid.

1. Introduction

The most common reasons to age either particulate or polymeric silica gels are to increase their strength prior to drying in order to avoid cracking and/or to alter the microstructure of the wet gel and subsequently the xerogel [1–4]. There are primarily three phenomena that occur during aging that can potentially contribute to strength increase or altered microstructure. (1) Silicate species can continue to attach to the gel network contributing to strength and stiffness [1]. (2) Condensation reactions may continue within the network, causing it to shrink and expel liquid in a process called syneresis [4]. (3) The pore fluid can react with the gel network, causing the

§ Parts I–III of this series appear in J. Non-Cryst. Solids 142 (1992) 189, 197 and 144 (1992) 32, respectively.

* Corresponding author. Tel: +1-505 277 2833. Telefax: +1-505 277 1024.

SSDI 0022-3093(93)E0239-S

replacement of surface groups and/or siloxane bond cleavage [2].

The processes of dissolution and reprecipitation are generally labeled coarsening or ripening [3,4], since solubility differences of surfaces with different radii of curvature, r, cause smaller particles to dissolve and to reprecipitate onto larger particles leading to larger and fewer particles; reprecipitation will also fill in crevices or necks between touching particles.

We expect that the kinetics of such reactions will depend on the local environment of the silicon, i.e., its extent of condensation. Due to the steric requirements of the pentacoordinate intermediate, the reaction rate should increase with a decrease in the number of bridging oxygen surrounding the silicon. In Q^n terminology (n is the number of bridging oxygens surrounding silicon) [4], the reaction rate should increase as $Q^4 < Q^3 < Q^2$. If the silicate particle or polymer is composed of a distribution of Q^n species, siloxane bond cleavage reactions may occur preferentially along 'paths of least resistance' defined by the Q^n distribution. For particulate silicates, this process could lead to roughened surfaces [4]. Conversely, if all the silicon species had identical environments, we expect uniform dissolution.

Repeated siloxane bond cleavage reactions lead to monomeric or oligomeric species, called 'soluble silicates' [3]. The soluble silicates can re-condense (re-precipitate) by the reverse reaction. This reaction has the same intermediate and hence the same steric requirements as the forward reaction [4]. The condensation reaction is minimal near the isoelectric point of silica ($\sim$ pH 2) and increases at both larger and smaller pH. In aqueous systems, re-precipitation occurs in a monomer-by-monomer fashion under reaction-limited conditions, leading to nearly dense silica. However, if the re-precipitation process involves oligomeric species or if it occurs under transport-limited conditions or preferentially on the most weakly condensed sites due to steric factors, the precipitated silica could be porous [4].

Mizuno and co-workers [5] aged silica gels in distilled water, 4N HCl or 2N NH_4OH and determined that both the surface area and tendency for cracking decreased as the pH of the aging fluid deviated from the isoelectric point (pH $\sim$ 2). Brinker and Scherer [6] prepared a multicomponent silicate gel at $\sim$ pH 2.5 and compared the microstructures that resulted after drying the samples aged in either the mother liquor or 3M NH_4OH. Base aging caused the average pore diameter of the xerogel to increase from about 2 to 25 nm and the bulk density to decrease from 1.27 to 0.72 g/cm^3. Glaves et al. [7] aged a two-step acid/base-catalyzed silica gel in ethanol or an ethanol/KOH mixture. After drying, the KOH-aged gel had a higher pore volume and lower surface area. However, the surface area of the aged wet gel prior to drying (determined using low-field NMR) was actually higher for the KOH-aged gels compared with the ethanol-aged gels [7]. The three sets of results [5–7] obtained for dry gels are consistent with the conventional view of a coarsening process driven by a reduction in the net curvature: elevated pH, where there is considerable silica solubility dissolution and re-precipitation, causes a surface area reduction, and a strengthening of the gel network. The stronger gel is less prone to crack and shrinks less during drying so it has larger pores and a lower density.

These studies provide information on the combined effects of aging and drying but fewer investigations address the influence of pH on the aging process alone. In one relevant study, Axelos et al. [8] used small angle X-ray scattering (SAXS) and zeta potential measurements to show that the surfaces of commercial particulate silica (Ludox HS) roughened when aged under basic conditions. At pH 7, the silica/water interface was abrupt as indicated by a Porod slope $P = -4$. At pH 10, the electron density profile of the silica/water interface was modeled by a Gaussian distribution [8]. The thickness of this density transition region was about 1.1 nm. The authors attributed this 'fuzzy' surface to a gel-like layer. Using SAXS to study the structure of Stöber silica spheres [9] with a range of sizes (diameter, 40–150 nm), van Helden et al. [10] observed feature sizes on the order of 1–3 nm. They could not conclusively state whether these features were pores within the particles (either uniformly spaced throughout the particle or at the particle surface) or artifacts

arising from SAXS de-smearing calculations. However, these features are on the same size scale as one might expect if Stöber spheres are formed via an aggregation process of primary particles (diameter < 10 nm), as has been previously suggested [11–14].

We have used a combination of in situ techniques including proton spin–lattice relaxation, SAXS and zeta potential to deduce the effect of pore fluid pH on the structure of colloidal silica particles during aging. We use ^{29}Si magic angle spinning-nuclear magnetic resonance (MAS-NMR), scanning and transmission electron microscopy (SEM, TEM) and conventional sorption studies to measure the dry products. We have investigated silica particles prepared by three routes, differing in Q^n distributions, Stöber silica spheres, Ludox and Cab-O-Sil. A comparison between data on these particulate silica results is made with observations for base aging of a two-step acid/base-catalyzed silica gel.

2. Experimental

Model monosized silica particles were obtained by the Stöber process [9]. By changing the water and ammonium hydroxide concentrations, the particle size was varied from 42 to 377 nm as determined by SEM measurements. After the sphere reaction was complete, the spheres were filtered, washed, redispersed and separated in a centrifuge to obtain a porous solid with high density (~ 37% porosity corresponding to a random dense packing), high coordination number, narrow distribution of coordination number and known particle diameters. Three commercial silica particles with differing chemical and physical properties were also used [3]. These include a colloidal silica (Ludox™ AS40) and two fumed silicas (Cab-O-Sil™ L90 and EH5). Silica gels were prepared via a two-step acid/base-catalyzed procedure as described by Brinker et al. [15] and commonly denoted as B2. First, tetraethyl orthosilicate (TEOS), ethanol, water and HCl (molar ratios 1:3:1:0.0007) were heated under constant reflux for 1.5 h. In the second step, 1 ml of 0.05M NH_4OH was added to 10 ml of the TEOS stock solution. The resulting mixture was then allowed to gel (~ 2 h) in 5 mm diameter NMR tubes and then was aged in the reaction liquid (mother liquor) for 22 h. In addition, a series of polydimethylsiloxanes [16] was prepared by mixing different volume fractions (~ 4–55 vol.%) in tetrahydrofuran (THF). Polymers with narrow molecular weight distribution over a wide molecular weight range (162–116 500) were used. These samples were placed in 5 mm NMR tubes and allowed to equilibrate thermally at 303 K for at least 2 h before low-field NMR spin–lattice relaxation measurements were performed [1].

To study the effect of aging fluid pH, the particulate solids and gels were aged in ethanol and/or water baths containing various quantities of HCl, KOH or NH_4OH. Gels, after the initial 22 h aging period in the mother liquor, were forced out of the NMR tubes and placed in an excess of aging fluid. After the last aging step, each sample was placed in a 5 mm or 7.5 mm NMR tube and allowed to equilibrate thermally at 303 K for at least 2 h. Surface area and pore structure of the wet samples were measured by low-field NMR spin–lattice relaxation measurements of the fluid as described previously [1]. Several comments regarding NMR-derived pore size distributions should be made. Pore sizes obtained from NMR are the hydraulic radius (V_p/A_s) which may vary significantly from other yardsticks of pore size such as an inscribed circle which one might obtain from thermoporometry or nitrogen condensation on a dried sample. Also, during the NMR experiment, diffusion occurs, leading to a degree of spatial averaging. The magnitude of this effect depends on both solvent diffusivity and NMR relaxation times (a function of pore size, solvent-surface chemistry, temperature and NMR field strength).

The zeta potential and surface charge density of various silica particles was calculated as a function of slurry pH from their electrophoretic mobility (a Matec ESA apparatus was used). Slurries of approximately 2 vol.% silica and 0.001M KCl as an electrolyte were employed.

After the NMR and zeta potential experiments were completed, samples were weighed, dried and re-weighed. Particle slurries were dried

at 373 K overnight. Gel samples aged in pure ethanol dried by means of a pin hole in the NMR tube caps. These caps were removed to dry samples aged in water. Gel samples were dried at 298 K for 5 days followed by 3 h at 373 K.

Nitrogen sorption at 77 K was used to obtain surface areas and pore volumes of dried samples. Samples were outgassed at 373 K and low pressure for at least 2 h prior to measurement. A five-point BET analysis ($0.05 < P/P_0 < 0.3$, N_2 molecular cross-sectional area = 0.162 nm^2) was conducted to obtain surface areas and a single condensation point ($P/P_0 = 0.995$) was used to determine the pore volumes. Adsorption measurements were made on single samples. Errors bars associated with these measurements were estimated from repeated measurements on similar samples in our laboratory. Skeletal densities were measured by helium displacement (Micromeritics 1330 pycnometer). Twenty repeat measurements were made for each sample. Thermal gravimetric analysis was performed in argon (Perkin–Elmer model 7 TGA) at a heating rate of 10 K/min. SEM microscopy was performed on coated samples (Hitachi S-800 field emission SEM), and TEM was performed on sectioned samples (Phillips CM-30 TEM).

MAS ^{29}Si spectra were recorded at 39.6 MHz (Chemagnetics console interfaced to a General Electric 1280 data station). A 7 mm diameter zirconia rotor was used to spin the sample at 5–6 kHz. High power 1H decoupling was applied during data acquisition. The RIDE pulse sequence [17] was used to reduce baseline roll. This sequence relies on the direct polarization of the observed nuclei; therefore, the resonance areas are expected to be proportional to concentration. Pulse delay times of 240 s were used to accumulate 256 free induction decays for the ^{29}Si spectra. This time is at least a factor of 6 longer than the estimated spin–lattice relaxation times of 35–40 s in air. Spectra were simulated assuming Gaussian components.

3. Results: particulate silica

High pH solutions are often used to promote dissolution/reprecipitation. As necks between smooth spherical particles grow, the specific surface area of the sample should decrease. To illustrate, 130 nm silica Stöber spheres were centrifuged in 5 mm NMR tubes to obtain ordered packing. Samples of the ordered packings were subsequently infiltrated with aqueous KOH solutions ranging in pH from 6.8 to 13.7. After aging for 24 h, surface areas were measured in solution for one sample at each pH by a NMR technique [7]. With increasing pH, we expect a decrease in the surface area as both solubility and dissolution rates increase. However, an increase in surface area (Fig. 1) is observed in the wet packing. Upon drying, the surface area of all samples is about 26 ± 2 m^2/g (note: the geometric surface area of spheres with diameter of 130 nm and assuming a density of 2.0 g/cm^3 is 23 m^2/g). Results for the slurries indicate a larger increase in surface area for a given pH (Fig. 1). In addition to the Stöber sphere slurry, slurries of Ludox AS-40, Cab-O-Sil L90 and Cab-O-Sil EH5 were aged under similar conditions. For the two Cab-O-Sil powders, the surface area was constant, within the errors of measurement by the NMR technique, for the entire pH range. An increase in surface area ($\sim 20\%$) at the highest pH was observed in the Ludox sample. The surface area of particles in the various samples increased in the following order after aging at pH 10: Cab-O-Sil < Ludox ≪ Stöber.

To understand the possible role of oligomers in contributing to the high surface areas measured at elevated pH, a series of (162 < molecular

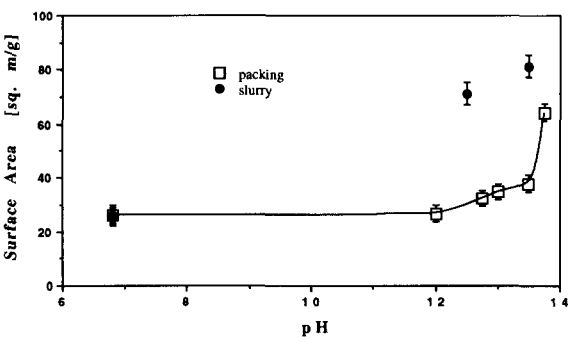

Fig. 1. Surface area of aged sphere packings and sphere slurry. The line is drawn as a guide for the eye.

weight (MW) < 116000) polysiloxanes with narrow molecular weight size distributions were measured by low-field NMR using THF as the solvent. Since the surface of these polymers is methylated rather than hydroxylated or ethoxylated and a different solvent is employed, the value of the NMR surface interaction parameter [1] ($\beta = 3.27$ nm/s) was found by performing a series of relaxation experiments on fumed silica with a methylated surface (Aerosil R-972) and measuring the surface area of the Aerosil by nitrogen adsorption. Within the limits of measurement error, we observed no MW dependence of surface area and even the lowest MW of 162 appears as surface area in the low-field NMR experiments. In order to ascertain what fraction of the observed surface area increase for the Stöber spheres is related to dissolved silica oligomers, the slurry at pH 13.6 was centrifuged (3400 rpm, 360 min) at ambient temperature and a spin–lattice relaxation experiment was performed on the supernatant. The difference in the T_1 of the supernatant and that of the aqueous KOH aging solution was less than errors in the data, thus, indicating no measurable change in the NMR properties of the fluid due to dissolved silica.

Following Axelos et al. [8], zeta potential and surface charge density measurements were made on the same silica particles as employed in the surface area measurements, with the exception that 270 nm diameter Stöber spheres were used instead of the 130 nm spheres described previously. The zeta potential, δ, and surface charge density, σ_0, determined at pH 7 and 10 are given in Table 1. As Axelos et al. have observed, the surface charge density increases for Ludox as the pH is increased. This effect is similar for the two Cab-O-Sil silicas but a larger increase is noted for the Stöber spheres. This surface charge density data parallels the low-field NMR surface area results described above.

The manufacturing processes for Cab-O-Sil, Ludox and Stöber silicas differ [3] and the differing effects of pH may be a result of the degree of silicon condensation resulting from the different manufacturing processes. Therefore, ^{29}Si MAS-NMR spectra were obtained for Cab-O-Sil (EH5), Ludox AS-40 and 270 nm Stöber spheres (see Fig. 2). Despite the lower surface area of the Stöber spheres, a larger fraction of Q^3 and Q^2 silicon atoms as compared with either Ludox or Cab-O-Sil was observed. In previous work, we have shown how the total surface area (i.e., accessible and inaccessible to nitrogen at 77 K) may be estimated from ^{29}Si MAS-NMR measurements using published values of OH and OR surface coverage [2]. Stöber spheres with four different diameters were synthesized with nominal (SEM) diameters of 42, 139, 191 and 377 nm. Assuming that the surface of the 42 nm spheres is covered with Si–OEt and that the three other spheres sizes primarily are covered with Si–OH (based on

Table 1
Variation of zeta potential, δ, and surface charge density, σ_0, as a function of pH. Surface area and zeta potential measurements are 5% and charge density measurements are 7%

	Surface area-dried (m^2/g)	δ (mV)		σ_0 (C/m^2)	
		pH = 7	pH = 10	pH = 7	pH = 10
Stöber-270 nm	15.8	−81.2	−154.2	−0.027	−0.122
Ludox AS-40	140	−74.9	−99.6	−0.024	−0.040
Cab-O-Sil L90	100	−51.4	−79.0	−0.014	−0.026
Cab-O-Sil EH5	380	−30.5	−61.3	−0.0074	−0.018

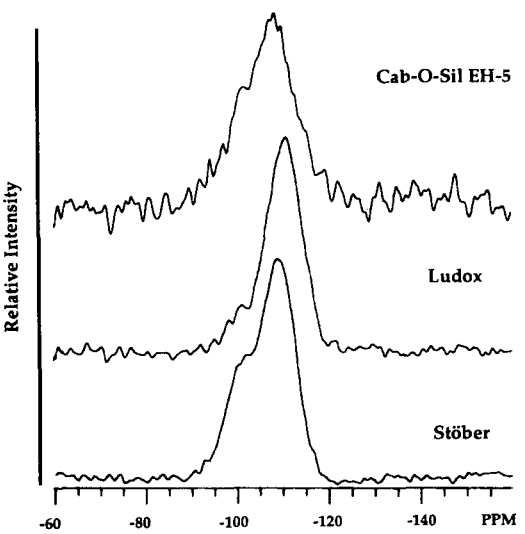

Fig. 2. ^{29}Si MAS-NMR spectra for Stöber spheres, Ludox and Cab-O-Sil EH5.

TGA analysis), surface areas can be calculated. These are compared with nitrogen adsorption-derived surface areas in Table 2. We should note that the low signal-to-noise of our ^{29}Si NMR spectra (Fig. 2) yields $\pm 10\%$ uncertainty in the NMR-derived surface areas. The differences between BET and Q surface areas indicates that the particles contain considerable internal surface area that is inaccessible to nitrogen at 77 K [2]. Assuming that the individual particles are actually aggregates of dense (2.2 g/cm^3) primary particles, we estimate the size of these primary particles from the Q distribution by assuming that the primary particles are uniform in size and that all terminated sites are located on the primary particle surface with a coverage of 4.7 OH/nm^2. From the Q surface area data, the primary particle size is ~ 4 nm for the three larger sphere sizes and ~ 2.5 nm for the smallest spheres. These sizes are in reasonable agreement with the predictions of Bogush and Zukoski [11,12] who calculated values of 3–6 nm for the primary particles in the larger sphere sizes. The assumption of smooth spheres which we employ implies that the primary particle sizes calculated from the silicon NMR results are a lower bound. In addition to surface area, skeletal densities were estimated from the Q distributions by assigning densities to both the siloxane and hydroxyl moieties. With the exception of the 42 nm particles, agreement, within errors of the data, between the helium and NMR-derived densities is observed. The lower

Table 2
Adsorption and NMR-derived properties as a function of particle size

SEM diameter (nm)	BET surface area (m^2/g) ±5%	'Q' surface area (m^2/g) ±10%	Helium density (g/cm^3) ±1%	'Q' density (g/cm^3) ±10%
42	369	1070	1.76	2.04
139	21.6	620	2.12	2.10
191	15.8	660	2.10	2.09
37	8.78	660	2.15	2.09

Table 3
Adsorption and ^{29}Si NMR-derived properties as a function of fluid aging conditions

SEM diameter (nm)	Aging pH	BET surface area (m^2/g) ±5%	'Q' surface area (m^2/g) ±10%
130	7	26.55	807
130	12	27.10	793
130	12.6	29.02	861
130	13	28.12	901

helium density for the 42 nm spheres is the result of ethanol/water which is trapped in the particles, causing a reduction in the density determined by helium pycnometry [2] (note: TGA indicates that this fluid evaporates between 573 and 673 K). ^{29}Si MAS-NMR on 130 nm spheres aged for 24 h at various pH indicate an increase in surface area with increasing pH (see Table 3). The silicon NMR results indicate that only a fraction of the total surface area of the spheres need be made accessible via base aging to explain the increase in surface charge density (Table 1) and low-field NMR surface area (Fig. 1).

Fig. 3 contains SEM micrographs of 270 nm spheres before and after aging in 0.5M KOH (pH = 13.6). A clear difference in surface morphology of the particles after aging can be observed. Features on length scales of 10–30 nm are noted on the surface of the aged spheres but the unaged spheres are smooth. These features are much larger than the primary size predicted by Bogush and Zukoski [11,12] and our Q surface areas.

The results presented above present no proof as to whether dissolution occurs at the sphere surface only in a thin microporous gel layer as proposed by Axelos et al. [8] or uniformly throughout the sphere. In an attempt to answer this, particles were aged for 24 h and placed in epoxy; thin sections ($\sim$ 90 nm) were prepared by microtoming and examined by TEM. A texture difference was noted between aged and unaged samples which we attribute to the penetration of KOH into the entire particle. Unlike the SEM results, no gradient in feature size or edge effects are apparent.

4. Discussion: particulate silica

The increase in *wet* surface area observed during aging at elevated pH could result from several processes including: (1) microporosity associated with the formation of necks between particles; (2) the presence of monomers/oligomers in solution resulting from dissolution that appear as 'surface' in the NMR surface area determination; or (3) the formation of a 'microporous gel' as suggested by Axelos et al. [8]. Comparing results obtained for slurries and sphere packings (Fig. 1), it is evident that the high surface areas are not attributable to neck formation: slurries that have few particle–particle contacts and greater surface areas exposed to the aging medium have higher wet surface areas after aging. NMR spin relaxation studies of the aging solution after centrifugation showed the contribution of oligomers (soluble silica) to the surface area to be negligible. Thus we are led to the conclusion that the surface area observed at high pH is attributable to a microporous gel region formed by partial hydrolysis of the silica framework. Further, combined zeta potential and ^{29}Si NMR experiments (Table 1 and Fig. 2) indicate that gel formation depends on the extent of condensation of the silica particles: after aging at pH 10, the increase in surface area increased as Cab-O-Sil < Ludox $\ll$ Stöber spheres, which is the reverse order of the corresponding extents of condensation. This observation is rationalized by consideration of the mechanism of siloxane bond hydrolysis (dissolution) [3,4]. The steric demands of the penta-coordinate intermediate should cause the hydrolysis rate to increase as bulky siloxane linkages are replaced by hydroxyl groups. This preference for hydrolysis at more weakly condensed sites leads to the formation of a high surface area microporous gel by an invasive process for Ludox and Stöber spheres, wheres Cab-O-Sil, which is composed of a uniform, fully condensed silica core, undergoes uniform dissolution with no associated roughening.

Despite the formation of a microporous gel in the wet state, the physical evidence acquired from the dried sphere packings is largely consistent with the conventional picture of ripening. For

example, we observe (1) a decrease in dry surface area with increasing pH (Fig. 4); (2) the formation of necks between particles (Fig. 3); and (3) a qualitative increase in strength with increasing pH. Thus it appears that, along with the formation of a gel region, there is a net removal of material from positive curvature surfaces and the deposition of material at negative curvature surfaces formed between touching spheres. During drying, capillary forces cause the collapse of the gel, quite effectively masking its existence in the wet state. The only possible evidence of the gel that survives in the dry state is a difference in contrast observed by SEM at the particle edges. This was observed for all aged spheres but not for any of the unaged spheres. This contrast difference could reflect a density difference arising from the formation of a gel and its collapse during drying.

5. Results: silica gel

For comparison with base aging of particulate silicas, changes in a silica gel aged under various pH conditions were studied. B2 gels were aged in aqueous HCl and KOH solutions to assess the effect of pore fluid pH on the pore structure of the wet gel. The surface areas in Fig. 4 and pore volumes in Fig. 5 were obtained by NMR or N_2 adsorption after aging in mother liquor for 22 h, immersion in aqueous aging solution (3 h for KOH and 24 h for HCl), washing in distilled water for 24 h and drying at 383 K. The pore size

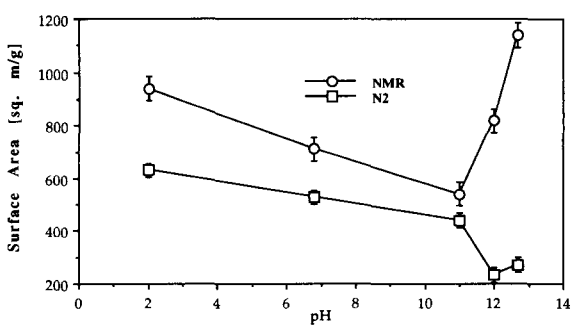

Fig. 4. Wet (NMR) and dry (N_2) surface areas as a function of aging pH. The lines are drawn as a guide for the eye.

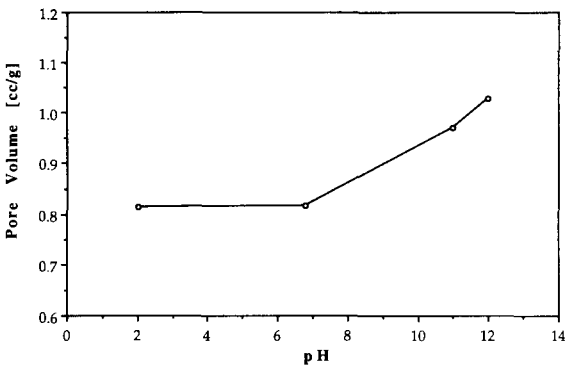

Fig. 5. Xerogel pore volumes prepared by aging (3 h), water washing and drying at 383 K. (Pore volume error bars are ± 0.01 cm^3/g.) The line is drawn as a guide for the eye.

distributions (PSD) of the wet gels were also obtained by NMR. From previous work in this series [2], simply placing gels in ethanol or water serves to narrow the PSD considerably. Fig. 6 shows that increasing the pH of the aqueous aging medium decreases the width of the PSD and, after aging for 3 h at pH 13, the PSD is narrower than that obtained with either temporal aging in the mother liquor for 359 h [1], thermal aging in mother liquor at 333 K [1] or aging in ethanol [2].

To evaluate any possible effect of monomer on either the NMR results or the base aging process itself, a second NMR experiment was performed in which the gels were washed in an excess of ethanol for 24 h prior to base aging. In addition to removing monomer, this 24 h washing in

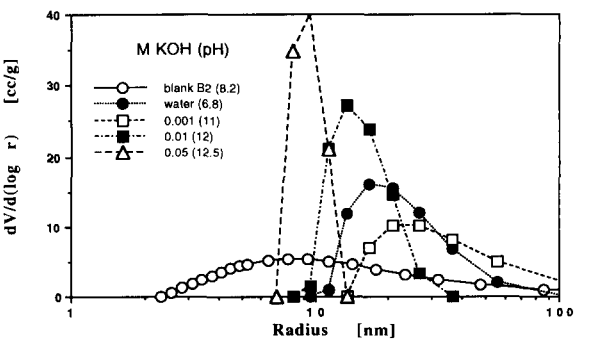

Fig. 6. Pore size distribution (PSD) of B2 gels after aging at various pH values for 3 h and washing in water. (Error bars on PSD are $\pm 5\%$.) The lines are drawn as a guide for the eye.

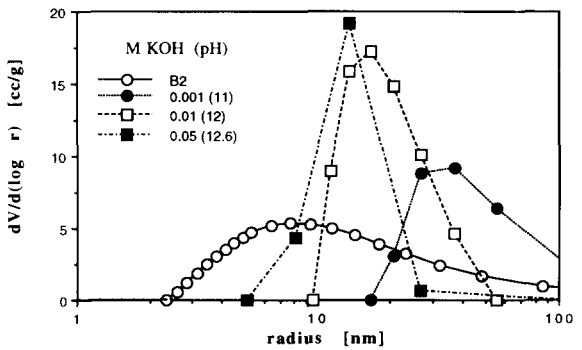

Fig. 7. PSD of B2 samples washed in ethanol, aged in KOH then washed in water. (Error bars on PSD are ±5%.) The lines are drawn as a guide for the eye.

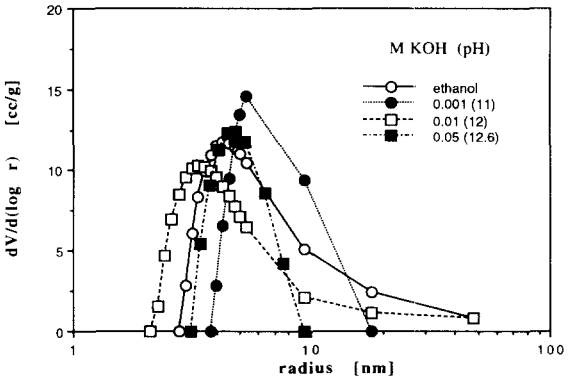

Fig. 9. PSD of gels washed in ethanol, base aged and washed in ethanol. (Error bars on PSD are ±5%.) The lines are drawn as a guide for the eye.

ethanol decreases the width of the PSD as described previously [2]. Fig. 7 shows that the trend of decreasing PSD width with increasing pH is still observed after this initial ethanol aging/washing process, but the decrease of PSD narrowing is less. Thus, these data show that the presence or absence of monomer does not have an effect on the overall aging process.

The use of water to remove the KOH can promote further hydrolysis, condensation and coarsening [2]. To reduce the possible effects due to water, samples were washed in ethanol (instead of water) after base aging. Fig. 8 shows the surface areas of these wet gels and corresponding xerogels. Fig. 9 presents the PSDs of the wet gels. Changing the final pore fluid from water to ethanol has been shown to increase both wet and dry surface areas [2]. This increase is attributed to partial depolymerization of the silica matrix in ethanol [2]. Since aging in pure ethanol depolymerizes the silica network and causes esterification of the newly created surfaces, the ethanol wash/base aging process is expected to increase the surface area and reduce the condensation rate. Thus, compared with results shown in Fig. 4 at each pH, larger surface areas are found for the samples washed in ethanol. As a result of the higher surface areas, ethanol aged samples have mean hydraulic radii (note: NMR pore sizes are the hydraulic radius, $=2V_p/A_s$) smaller than samples aged in water (compare Figs. 6 and 9). The PSDs in Fig. 9 agree with Figs. 6 and 7 in that the narrowest PSD is obtained at the highest pH even though the extent of further condensation or coarsening after base aging was reduced.

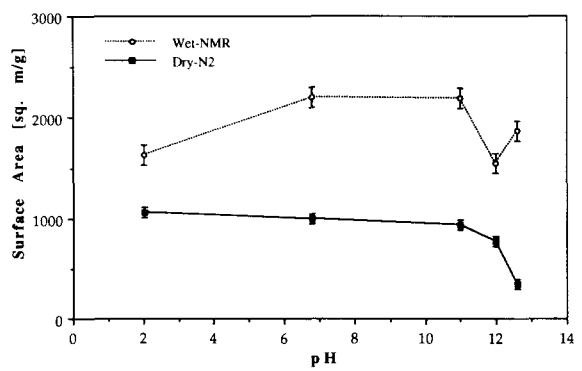

Fig. 8. Gel surface area after ethanol wash, KOH aging and ethanol washing. The lines are drawn as a guide for the eye.

The effect of time of the base aging process was investigated by aging samples in the most basic solution studied (pH 12.6) for various periods of time, washing in either water or ethanol for 24 h and drying. Fig. 10 shows both the NMR (wet) and N_2 (dry) surface areas of these samples.

The pore volumes obtained from N_2 condensation for the samples aged at pH 12.6 as a function of time washed in either water or ethanol and dried are presented in Fig. 11. As an Ostwald ripening mechanism would predict, the pore volume increases with increased base aging times for samples washed and dried in water or ethanol,

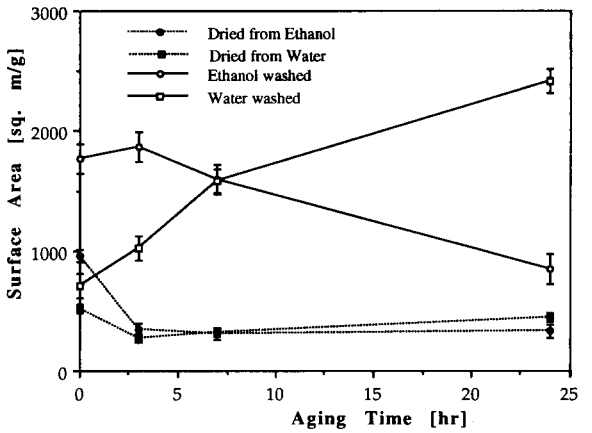

Fig. 10. Wet (NMR) and dry (N_2) surface areas for B2 gels as a function of base aging time. The lines are drawn as a guide for the eye.

although the pore volumes for samples dried from ethanol are all larger then those dried from water. The increased condensation that occurs during water washing leads to a stiffer matrix as observed for similar B2 gels [18] but this increased matrix rigidity is offset by the higher capillary pressure resulting from the much higher surface tension of water (22 vs. 72 dyn/cm). The effect of surface tension on capillary pressure-induced collapse during drying has been demonstrated by Deshpande and et al. [19].

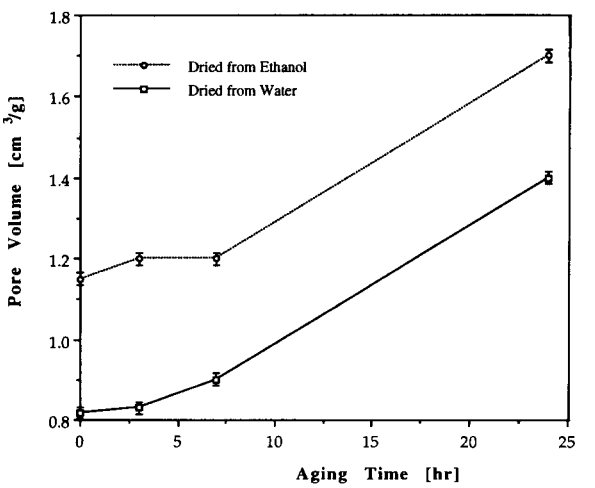

Fig. 11. Xerogel pore volume as a function of base aging time at pH = 12.6. (Error bars on pore volume are ± 0.01 cm^3/g.) The lines are drawn as a guide for the eye.

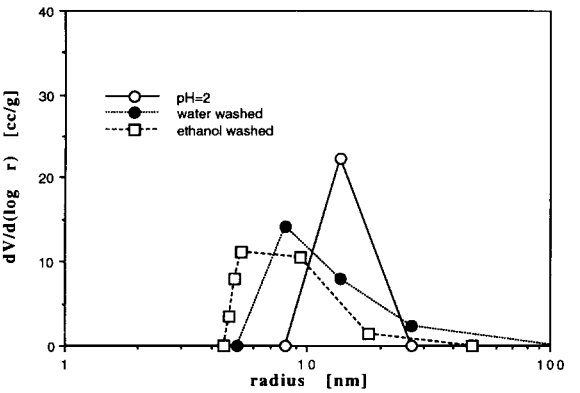

Fig. 12. PSDs of B2 gels aged at the isoelectric point. The lines are drawn as a guide for the eye.

Pore size distributions of gels aged at the isoelectric point were obtained by aging a B2 gel for 22 h in mother liquor, immersing it in an aqueous HCl solution of pH 2 for 24 h, performing a NMR spin–lattice relaxation experiment and then washing out the acid by placing the gel in either water or ethanol for 24 h. Fig. 12 shows these PSDs. The water-washed sample has a larger mean pore size then the ethanol-washed sample, and both PSDs are somewhat broader than that obtained prior to washing. The corresponding xerogel surface area for the sample dried from water is lower (630 m^2/g) than that of the sample dried from ethanol (1054 m^2/g). In fact, the acidic aging had little effect on the final pore structure achieved (the pore volumes were also similar to those for gels simply aged in ethanol or water at pH 7).

6. Discussion: silica gel

The high surface area of a wet gel or xerogel at the isoelectric point (pH = 2) could be due to the fact that the condensation rate is minimal at this pH [4] as well as the fact that the dissolution rate is low. These effects should serve to reduce dissolution/reprecipitation [3] and thus lead to weakly condensed gels characterized by higher surface areas. As pH is increased, the dissolution

and condensation rates are also increased [3]; thus the surface area decreases linearly with pH. In highly basic solutions, the trend is reversed for wet gels and a sharp increase in surface area is seen for pH = 11. The surface area increase in these base solutions is attributed to the same mechanisms as that proposed for the colloidal sphere packings, i.e., the exposure of additional internal surface within the matrix due to removal of low coordination silicon and an increase in the oligomer concentration. Upon drying, the surface area (Fig. 4) and pore volume (Fig. 5) follow the trend predicted by Ostwald ripening. After drying, base-aged samples washed in water and those washed in ethanol both have low surface areas of about 250 m^2/g regardless of the time allowed for base aging or the solvent used to remove the KOH base. However, prior to drying, the surface area depends on the final solvent used. As the aging time increases, so does the degree of dissolution of the silica matrix.

Upon introduction of ethanol or water to remove the KOH, the silica present in the pore fluid can either be exchanged with pure solvent or react with it. Introduction of pure ethanol will esterify the matrix as well as the dissolved silica species, thus eliminating condensation. The introduction of water will hydrolyze the matrix and silica in the pore fluid, thus promoting condensation. The hydrolyzed silica species in solution may be added to the matrix or combine with other dissolved silica species before attaching to the silica matrix. This will result in a stiffer matrix which is better able to resist collapse during drying.

7. Conclusions

The study of Ostwald ripening during aging of particulate silica or silica gel at high pH is complicated by concurrent siloxane bond hydrolysis at less highly condensed silicon centers and the possible presence of oligomers that cause the surface area in the wet state to increase. However, continued aging at high pH yields a stiffer network with larger pores and a narrower pore size distribution. Therefore, in the final dried state, a larger pore volume and lower surface area is obtained.

This work has been supported by Sandia National Laboratories (#05-5795). One of the authors (P.J.D.) has been partially supported by a New Mexico Fellowship for Underrepresented Groups in Science. The authors thank the following UNM/NSF CMEC researchers: G. Johnston for nitrogen adsorption analysis, S. Thoma for the Stöber sphere synthesis and S. Hietala for SEM measurements. The help of G. Bogush of Sandia National Laboratories who performed the zeta potential measurements and E. Boyes of DuPont for the TEM results is greatly appreciated. Discussions with G. Scherer of DuPont contributed significantly to this work.

References

[1] P.J. Davis, C.J. Brinker and D.M. Smith, J. Non-Cryst. Solids 142 (1992) 189.
[2] P.J. Davis, C.J. Brinker, D.M. Smith and R.A. Assink, J. Non-Cryst. Solids 142 (1992) 197.
[3] R.K. Iler, The Chemistry of Silica (Wiley, NY, 1979).
[4] C.J. Brinker and G.W. Scherer, Sol–Gel Science (Academic Press, NY, 1989).
[5] T. Mizuno, H. Nagata and S. Manabe, J. Non-Cryst. Solids 100 (1988) 236.
[6] C.J. Brinker and G.W. Scherer, in: Ultrastructure Processing of Ceramics, Glasses, and Composites, ed. L.L. Hench and D.R. Ulrich (Wiley, New York, 1984) p. 43.
[7] C.L. Glaves, C.J. Brinker, D.M. Smith and P.J. Davis, Chem. Mater. 1 (1989) 34.
[8] M.A.V. Axelos, D. Tchoubar and J.Y. Bottero, Langmuir 5 (1989) 1186.
[9] W. Stöber, W. Bohn and A. Fink, J. Colloid Interf. Sci. 26 (1968) 62.
[10] A.K. van Helden, J.W. Jansen and A. Vrij, J. Colloid Interf. Sci. 81 (1981) 354.
[11] G.H. Bogush and C.F. Zukoski, J. Colloid Interf. Sci. 142 (1991) 1.
[12] G.H. Bogush and C.F. Zukoski, J. Colloid Interf. Sci. 142 (1991) 19.
[13] J. Bailey and M. Mecartney, in: Better Ceramics Through Chemistry IV, Materials Research Society Conf. Proc. Vol. 153, ed. B.J.J. Zelinski, C.J. Brinker, D.E. Clark and D.R. Ulrich (Materials Research Society, Pittsburgh, PA, 1990) p. 153.
[14] A.J. LeCloux, J. Bronckart, F. Noville, C. Dodet, P. Marchot and J.P. Pirard, Colloids Surf. 19 (1986) 359.

[15] C.J. Brinker, K.D. Keefer, D.W. Schaefer and C.S. Ashley, J. Non-Cryst. Solids 48 (1982) 47.
[16] R. Anderson, B. Arkles and G.L.Larson, Petrarch Systems: Silicon Compounds, Register and Review (Petrarch Systems, Bristol, PA, 1987) p. 259.
[17] P.S. Belton, I.J. Cox and R.K. Harris, J. Chem. Soc. Faraday Trans. 81 (1985) 63.
[18] R. Deshpande, PhD dissertation, University of New Mexico (1992).
[19] R. Deshpande, D.M. Smith and C.J. Brinker, J. Non-Cryst. Solids 144 (1992) 32.